Progress In Electromagnetics Research C, Vol. 33, 213–227, 2012

MAXIMUM BANDWIDTH PERFORMANCE FOR AN IDEAL LUMPED-ELEMENT CIRCULATOR

H. Dong*, J. L. Young, J. R. Smith, and B. Aldecoa

Department of Electrical & Computer Engineering, University of Idaho, P. O. Box 441023, Moscow, ID 83844-1023, USA

Abstract—A procedure based on the analytical model of a lumped-element, crossover circulator has been developed to maximize its operating bandwidth. The procedure considers the circulator as a network and employs the circulation impedance — the load associated with perfect circulation — as a metric to optimize the bandwidth. Using this procedure, we find that a maximum 194% bandwidth can be obtained for an ideal circulator for above-FMR operation. When the same procedure is applied using a simulation model for the 225–400 MHz frequency range, we achieve 125% bandwidth. We have verified this result from the measurement of a fabricated device; the measured data reveals a bandwidth of 129%.

1. INTRODUCTION

Research on lumped-element, crossover circulators for RF communication applications commenced in the early 1960's with the work of Konishi [1], who articulated the theory of operation for the UHF and VHF band. Soon thereafter considerable effort was expended on both the crossover network and the matching network to widen its bandwidth [2, 3]. In recent years a resurgence of activity in crossover circulator research has occurred due to the advances in mobile communication devices.

Among the circulator's many important properties, large bandwidth is one of the most important. This leads us to the question of how much bandwidth a crossover circulator can achieve. Miura et al. [4] provided one answer using an eigenvalue analysis and reported a 9.8% bandwidth (820–900 MHz) for miniature circulators. Schloemann [5] provided a different perspective on bandwidth by

Received 23 August 2012, Accepted 12 October 2012, Scheduled 16 October 2012

* Corresponding author: Hang Dong (dong4104@vandals.uidaho.edu).

relating bandwidth performance to the geometric design of the ferrite crossover network. Using a quality factor analysis, he showed that bandwidths on the order of one and two octaves are possible, but no simulation or experimental results support this claim. A casual review of circulators currently on the market indicates that the current state-of-the-art is close to 100% for operating frequencies near 400 MHz.

In this paper we are interested in determining the upper bound on bandwidth based upon theoretical considerations and optimization methodologies. Particularly, using the concept of the circulation impedance, which refers to the impedance load that results in perfect isolation, in conjunction with an ideal electromagnetic field model, we find that a 194% maximum bandwidth is theoretically possible. This result is independent of the choice of center frequency for above-FMR (ferromagnetic resonance) operation. Using more precise models as obtained from simulation and typical values for the magnetic saturation, we show that bandwidths on the order of 130% are realistic. This latter result is also confirmed by experimentation.

In the following sections we provide some perspectives on the optimization process and show how the notion of the circulation impedance can be used to estimate device bandwidth. A theoretical treatment, simulation data, and measurement data are provided to support the claims made herein.

2. THEORETICAL ANALYSIS

2.1. Ideal Model

We start our analysis with the ideal network model of a lumped-element, crossover circulator that was developed by Bergman [6]. The basic configuration of a crossover circulator, which is shown in Figure 1,

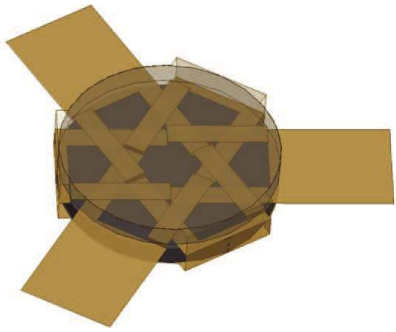

Figure 1. A typical lumped-element, crossover ferrite circulator.

consists of two ferrite pucks with three conductor traces between them. The ferrite pucks are assumed to be fully saturated by an external biasing field H_a whose direction is perpendicular to the trace plane. The traces are placed at 120° intervals to form a crossover topology. All three traces are assumed to be electrically isolated from each other using air as an insulator. One end of any trace is used as the port of the circulator while the other end is connected to the ground plane that forms the housing of the structure (not shown for clarity). This circulator device forms a three-port network. When one assumes that the internal RF field is uniform, the Z-parameters of the ideal device can be expressed as [6]

$$\begin{aligned} Z_{11} &= Z_{22} = Z_{33} = j\omega L_0 \mu \\ Z_{12} &= Z_{23} = Z_{31} = -j\omega L_0(\mu - j\sqrt{3}\kappa)/2 \\ Z_{13} &= Z_{21} = Z_{32} = -j\omega L_0(\mu + j\sqrt{3}\kappa)/2, \end{aligned} \tag{1}$$

where L_0 is an effective inductance for each port and is defined by

$$L_0 = \frac{\mu_0 A_e}{l_e}. \tag{2}$$

Here A_e and l_e are effective area and length parameters that satisfy the dimensionality requirements of the previous equation. The effective area is related to the trace area and the effective length to the trace width, but their precise values are not needed at this time. However, since A_e and l_e are only dependant on the physical dimensions of the ferrite pucks and traces, L_0 is a function of the geometrical layout of the device. The other two parameters in Eq. (1), μ and κ, characterize the ferrite material and are defined by [7]

$$\mu = 1 + \frac{\omega_0 \omega_m}{\omega_0^2 - \omega^2} \tag{3}$$

and

$$\kappa = \frac{\omega_m \omega}{\omega_0^2 - \omega^2}. \tag{4}$$

Here ω_m is associated with the magnetic saturation of the ferrite such that $\omega_m = 2\pi f_m$, where $f_m = (2.8 \times 10^6)(4\pi M_s)$ (Hz/G). Also, ω_0 is the Larmor angular frequency, which is a function of the internal field H_0 of the ferrite disks through the relationship $\omega_0 = 2\pi f_0$, where $f_0 = (2.8 \times 10^6)(H_0)$ (Hz/Oe). The internal field H_0 is a function of both the external biasing field H_a and the demagnetization field. For non-ellipsoidal shapes (i.e., disks), the demagnetization field is computed from a tensor demagnetization factor. For purposes of the study, we make the usual assumption that the demagnetization tensor is well approximated by a scalar such that

$$H_0 \approx H_a - 4\pi M_s N_z, \tag{5}$$

where N_z is the demagnetization scalar in the z direction. Although N_z is technically a function of position, we treat it as a constant in the context of the ideal model. The pros and cons of this assumption have been discussed extensively in [12–14]. For thin disks, $N_z \approx 1$ [15]. For above-FMR operation ω_0 defines the upper frequency limit of the operating range. When ω nearly equals $\omega_\circ$ the losses in the ferrite are excessive and the fields tend to be evanescent.

The Polder terms μ and κ defined in Eqs. (3) and (4) are written for lossless ferrites. When ferrite loss is considered, we replace ω_0 with $\omega_0 + j\alpha\omega$, where α is a phenomenological loss coefficient calculated from the linewidth of the ferrite material. For actual ferrites operating in above-FMR mode, linewidths as small as 10 Oe are available, resulting in values of α less than 10^{-3}. It is therefore reasonable to assume no loss in our initial theoretical analysis of an ideal circulator. Moreover, since loss tends to increase bandwidth, we choose to set $\alpha = 0$ in order to create a least upper bandwidth bound.

By inserting Eqs. (3) and (4) into (1), we obtain the following impedance parameters:

$$\begin{aligned} Z_{11} &= j\omega L_0 \left(1 + \frac{\omega_0\omega_m}{\omega_0^2 - \omega^2}\right) \\ Z_{21} &= -\frac{Z_{11}}{2} + \frac{\sqrt{3}}{2}\left(\frac{\omega^2\omega_m L_0}{\omega_0^2 - \omega^2}\right) \\ Z_{31} &= -\frac{Z_{11}}{2} - \frac{\sqrt{3}}{2}\left(\frac{\omega^2\omega_m L_0}{\omega_0^2 - \omega^2}\right). \end{aligned} \tag{6}$$

These equations can be rewritten as

$$\begin{aligned} Z_{11} &= jX \\ Z_{21} &= -j\frac{1}{2}X + R \\ Z_{31} &= -j\frac{1}{2}X - R \end{aligned} \tag{7}$$

with

$$R = \frac{\sqrt{3}\omega L_0}{2}\left(\frac{\omega\omega_m}{\omega_0^2 - \omega^2}\right) \tag{8}$$

and

$$X = \omega L_0 \left(1 + \frac{\omega_0\omega_m}{\omega_0^2 - \omega^2}\right). \tag{9}$$

These latter forms for Z_{ij} will simplify the ensuing mathematical manipulations.

2.2. Circulation Impedance and Bandwidth Estimation

From a three-port network point of view the circulation impedance Z_c is defined as the load that results in perfect isolation [10]. This same load will also result in perfect return loss and insertion loss when the network is lossless. The combined result is called perfect circulation. According to [10], when port one is chosen as the input and port three is isolated, the load impedance at port two must be of the form

$$Z_c = \frac{Z_{32}Z_{21}}{Z_{31}} - Z_{22}. \tag{10}$$

For the three-port symmetrical crossover network whose Z-parameters are given by Eqs. (7), (8) and (9), this load impedance is also used for the other two ports. In terms of R and X, we replace the previous equation with

$$Z_c = \frac{Z_{21}^2}{Z_{31}} - Z_{11} = \left(R - j\frac{1}{2}X\right)\left(\frac{3X^2 - 4R^2}{X^2 + 4R^2}\right). \tag{11}$$

Typically, perfect circulation is achievable at a few discrete frequencies and partially achieved over a range of frequencies, say from f_a to f_b. The bandwidth BW is defined using specified values of isolation I, return loss RL, and insertion loss IL over the range f_a to f_b. For purposes herein we arbitrarily regard 15 dB of isolation and return loss along with 0.5 dB of insertion loss as acceptable when discussing bandwidth. The following bandwidth metric relative to f_a will be used:

$$\%\ BW \equiv \frac{f_b - f_a}{f_a} \times 100\%. \tag{12}$$

Such a definition allows us to say that one octave or 100% corresponds to the same bandwidth.

A typical plot of Z_c normalized by $\omega_0 L_0$ is shown in Figure 2. To realize Z_c a lossless matching network needs to be placed between the crossover device and the load resistor R_L to transform R_L into Z_c. How well such a matching network can accomplish this task dictates the operating bandwidth. It is obvious from Figure 2 that if perfect circulation performance is desired in the range $0 < f < f_0$, a load with negative reactance is needed. To realize this negative reactance of Z_c it behooves us to use a shunt capacitor C_0 across each port. Also, it is well known that a capacitor C_g placed between the common wire of the ports and the ground of the circulator can widen the operating bandwidth [8, 9]. According to Knerr, tuning components connected to the ports can only affect two of the three eigenvalues of the three-port network while C_g can influence the third eigenvalue. Hence, this eigenvalue analysis appeals to the optimal topology of the tuning

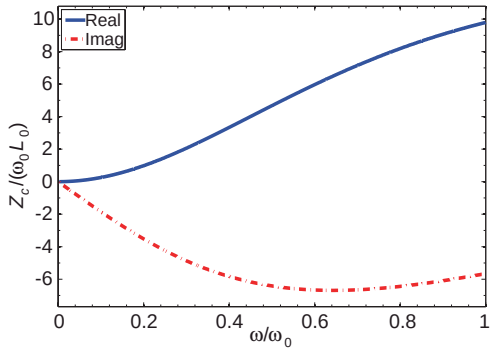

Figure 2. Typical Z_c data of an ideal circulator; here $\omega_m/\omega_0 = 4$.

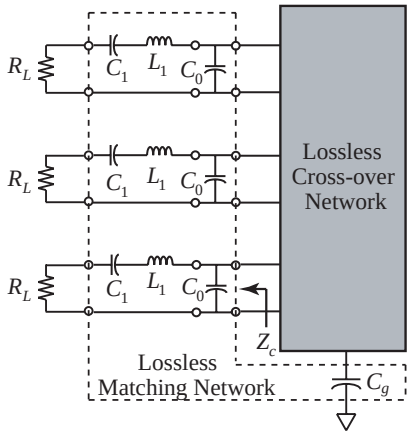

Figure 3. Matching network realization of Z_c.

network, as shown in Figure 3. The role of L_1 and C_1 will be discussed in an ensuing paragraph.

The precise effect of C_0 and C_g can be understood through the following analysis. We start with the normalization of the impedance matrix $\mathbf{Z}$ of the ideal crossover network:

$$\mathbf{N} \equiv \frac{\mathbf{Z}}{\omega_0 L_0} = \begin{bmatrix} N_{11} & N_{31} & N_{21} \\ N_{21} & N_{22} & N_{31} \\ N_{31} & N_{21} & N_{33} \end{bmatrix} \tag{13}$$

where

$$N_{11} = \frac{Z_{11}}{\omega_0 L_0} = j\bar{X}, \tag{14}$$

$$N_{21} = \frac{Z_{21}}{\omega_0 L_0} = -j\frac{1}{2}\bar{X} + \bar{R}, \tag{15}$$

and

$$N_{31} = \frac{Z_{31}}{\omega_0 L_0} = -j\frac{1}{2}\bar{X} - \bar{R}, \tag{16}$$

in which case

$$\bar{R} = \frac{R}{\omega_0 L_0} = \frac{\sqrt{3}}{2}\left[\frac{(\omega/\omega_0)^2(\omega_m/\omega_0)}{1-(\omega/\omega_0)^2}\right] \tag{17}$$

and

$$\bar{X} = \frac{X}{\omega_0 L_0} = \frac{\omega}{\omega_0}\left(1 + \frac{\omega_m/\omega_0}{1-(\omega/\omega_0)^2}\right). \tag{18}$$

By placing C_0 across each port, the crossover network is transformed into a new network whose Z-parameter matrix is $\mathbf{Z}'$; the relationship between $\mathbf{Z}$ and $\mathbf{Z}'$ is

$$\mathbf{Z}' = [\mathbf{U} + j\omega C_0 \mathbf{Z}]^{-1}\,\mathbf{Z} = \omega_0 L_0\,[\mathbf{U} + j\omega C_0 \omega_0 L_0 \mathbf{N}]^{-1}\,\mathbf{N}. \tag{19}$$

Here, $\mathbf{U}$ is the identity matrix. If we define

$$\omega_r \equiv \frac{1}{\sqrt{L_0 C_0}} \tag{20}$$

as the resonant frequency related to C_0 and L_0, through various manipulations, $\mathbf{Z}'$ can be equally written as

$$\mathbf{Z}' = \omega_0 L_0 \left[\mathbf{U} + j\frac{(\omega/\omega_0)}{(\omega_r/\omega_0)^2}\mathbf{N}\right]^{-1}\mathbf{N}. \tag{21}$$

Applying similar normalizations as in Eq. (13) to $\mathbf{Z}'$, we obtain

$$\mathbf{N}' \equiv \frac{\mathbf{Z}'}{\omega_0 L_0} = \left[\mathbf{U} + j\frac{(\omega/\omega_0)}{(\omega_r/\omega_0)^2}\mathbf{N}\right]^{-1}\mathbf{N}. \tag{22}$$

When C_g is connected to the network, the Z-parameters are transformed from $\mathbf{Z}'$ into $\mathbf{Z}''$ such that

$$\mathbf{Z}'' = \mathbf{Z}' + \frac{1}{j\omega C_g}\mathbf{E} = \omega_0 L_0\left(\mathbf{N}' + \frac{1}{j\omega_0 \omega L_0 C_g}\mathbf{E}\right) \tag{23}$$

where

$$\mathbf{E} = \begin{bmatrix} 1 & 1 & 1 \\ 1 & 1 & 1 \\ 1 & 1 & 1 \end{bmatrix}. \tag{24}$$

If we define ω_g as the grounding resonant frequency associated with C_g and L_0 by

$$\omega_g \equiv \frac{1}{\sqrt{L_0 C_g}}, \tag{25}$$

then $\mathbf{Z}''$ becomes

$$\mathbf{Z}'' = \omega_0 L_0 \left(\mathbf{N}' - \frac{j(\omega_g/\omega_0)^2}{(\omega/\omega_0)} \mathbf{E} \right). \tag{26}$$

Again, it is desirable to normalize $\mathbf{Z}''$ and write

$$\mathbf{M} \equiv \frac{\mathbf{Z}''}{\omega_0 L_0} = \left(\mathbf{N}' - \frac{j(\omega_g/\omega_0)^2}{(\omega/\omega_0)} \mathbf{E} \right). \tag{27}$$

By definition $\mathbf{M}$ is the normalized Z-parameter matrix of the crossover network together with C_0 and C_g tuning. Although C_0 and C_g are part of the matching network, we refer to them as "tuning elements" since their function is to shift the center frequency to the desired frequency band. The normalized circulation impedance Z_{cm} for this transformed network, per Eq. (10), is therefore

$$\frac{Z_{cm}}{\omega_0 L_0} = \frac{M_{21}^2}{M_{31}} - M_{11}. \tag{28}$$

From Eqs. (13), (22) and (27), we can see that $\mathbf{M}$ depends on four frequency ratios:

$$\frac{\omega}{\omega_0}, \ \frac{\omega_m}{\omega_0}, \ \frac{\omega_r}{\omega_0}, \text{ and } \frac{\omega_g}{\omega_0}.$$

Moreover, since $Z_{cm}/(\omega_0 L_0)$ is a function of the matrix elements of $\mathbf{M}$, it is only controlled by these four ratios. For a given set of parameters $Z_{cm}/(\omega_0 L_0)$ can be calculated and the operating bandwidth for the corresponding device can be estimated.

Consider a typical plot of $Z_{cm}/(\omega_0 L_0)$ as shown in Figure 4. After including the tuning elements C_0 and C_g, our goal is to find a matching network that can transform the resistive load R_L into Z_{cm}. This can

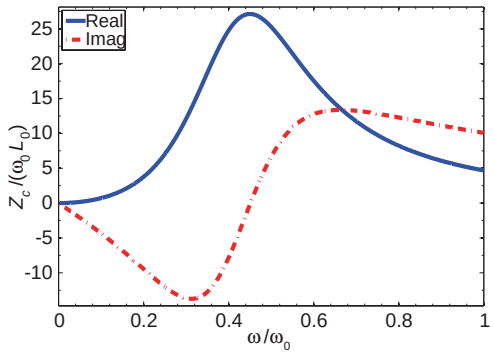

Figure 4. A typical plot of Z_c with C_0 and C_g tuning.

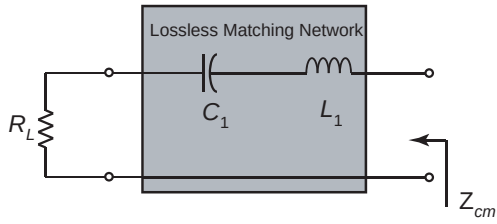

Figure 5. The matching network topology for a post-tuned crossover network.

be accomplished using a series LC circuit, which is shown in Figure 5. A comparison between Z_{cm} and the impedance Z_{Mat} of this series LC circuit and resistive load shows that in the frequency range f_a to f_b good agreement is obtained (see Figure 6). The imaginary part of Z_{Mat} matches the circulation reactance X_{cm} (i.e., the imaginary part of Z_{cm}) very well while the real part of Z_{Mat}, which is just the load R_L, matches the circulation resistance R_{cm} (i.e., the real part of Z_{cm}). From the definition of circulation impedance it is clear that near-perfect circulation is achieved in the range f_a to f_b by having this matching network connected between the crossover network and R_L on each port, even though R_{cm} is not perfectly matched with R_L. The mismatch between R_L and R_{cm} determines the value of isolation since the match between X_{Mat} and X_{cm} is nearly perfect. For example, 14 dB of isolation suggests that R_L should be set to around 2/3 of the peak value of R_{cm}.

Since we have circulation over the range f_a to f_b, the frequencies f_a and f_b are the estimated bounds for the band of operation. These frequencies, as discussed previously, are the zero slope points of X_{cm}. However, if the maximum of X_{cm} occurs outside of the range $[0,\ f_0]$, we set $f_b = f_0$ to avoid operating near resonance. As an example, consider Figure 6 in which $\omega_a/\omega_0 = 0.312$ and $\omega_b/\omega_0 = 0.664$; for this case $BW = 112\%$.

2.3. Bandwidth Optimization

The preceding analysis reveals how the normalized circulation impedance $Z_{cm}/(\omega_0 L_0)$ of the network is a function of the four frequency ratios ω/ω_0, ω_m/ω_0, ω_r/ω_0 and ω_g/ω_0. And since bandwidth is estimated from the circulation impedance, it is therefore determined by these four ratios. This suggests that optimal values for these ratios exist that maximize bandwidth over the range $0 < \omega/\omega_0 < 1$. The details of the optimization method are not the subject of this paper, but

the results are. We found through an exhaustive search methodology that the following design results in the widest bandwidth:

$$\begin{aligned} \omega_m/\omega_0 &= 118 \\ \omega_r/\omega_0 &= 8.7 \\ \omega_g/\omega_0 &= 2 \\ f_a/f_0 &= 0.34 \\ f_b/f_0 &= 1.00 \\ BW &= 193.8\%. \end{aligned} \tag{29}$$

Therefore, based on the ideal model, bandwidths near 200% are technically achievable. Whether an actual circulator can achieve such high bandwidth values is the subject of the ensuing discussion. In fact, we believe that the optimal value of ω_m/ω_0 approaches infinity, albeit very slowly, in the search algorithm with almost no change in the bandwidth result.

By using the normalized Z-parameters of the crossover network in Eqs. (13), (22) and (27), we can choose any frequency band of interest. For our research we are interested in the frequency range 225–400 MHz and set $\omega_0 = 800\pi\,\mathrm{r/s}$ along with $L_0 = 1\,\mathrm{nH}$. From the ratios of Eq. (29), we find that

$$\begin{aligned} 4\pi M_s &= 16,857\ \mathrm{G} \\ C_0 &= 2.1\,\mathrm{pF} \\ C_g &= 39.6\,\mathrm{pF} \\ f_a &= 136\,\mathrm{MHz} \\ f_b &= 400\,\mathrm{MHz} \\ BW &= 193.8\%. \end{aligned} \tag{30}$$

Figure 7 shows a plot of $Z_{cm}/(\omega_0 L_0)$ for this design. If we constrain $4\pi M_s$ to a realizable value for practical applications (e.g., $4\pi M_s = 2,000\,\mathrm{G}$), a 180% maximum bandwidth is still achieved for the design frequency range. The results for this case are

$$\begin{aligned} 4\pi M_s &= 2,000\,\mathrm{G} \\ C_0 &= 16\,\mathrm{pF} \\ C_g &= 323\,\mathrm{pF} \\ f_a &= 143\,\mathrm{MHz} \\ f_b &= 400\,\mathrm{MHz} \\ BW &= 180\%. \end{aligned} \tag{31}$$

With the optimal crossover network so determined, the last step is to calculate the value of the matching components C_1 and L_1. The

components C_1 and L_1 approximate the circulation reactance X_{cm} through resonance. They can be estimated by recognizing that the slope of X_{Mat} through resonance is $2L_1$; from this value and the resonant frequency, C_1 can be estimated. That is,

$$L_1 \approx \frac{1}{2}\frac{X_{cm\_b} - X_{cm\_a}}{2\pi(f_b - f_a)} \tag{32}$$

and

$$C_1 = \frac{1}{(2\pi f_r)^2 L_1}, \tag{33}$$

where X_{cm_a} and X_{cm_b} are values of the circulation reactance at frequencies f_a and f_b, respectively, and f_r is the frequency at which X_{cm} crosses zero. Also, as mentioned before, the load R_L is estimated

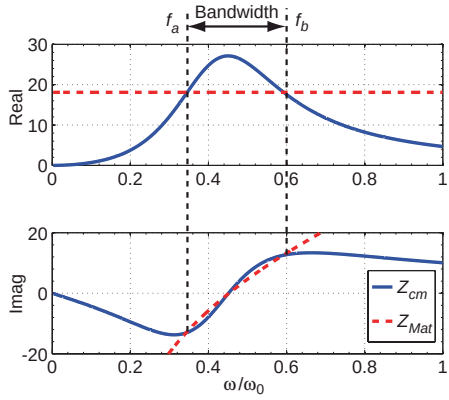

Figure 6. Comparison of Z_{cm} and the impedance of a series RLC circuit.

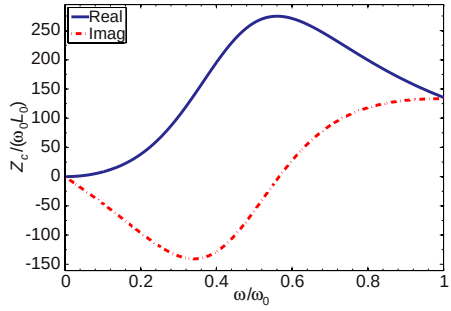

Figure 7. A plot of $Z_{cm}/(\omega_0 L_0)$ verses frequency for the widest bandwidth performance design when $f_b = 400\,\text{MHz}$.

to be 2/3 of peak value of R_{cm} for a 14 dB isolation and return loss. These estimations for L_1, C_1 and R_L are excellent seed values when searching for the optimal values. An optimization algorithm is invoked that uses this set of seed values and employs the Pareto Front population analysis [11] to find the optimal set. The optimization method is based on the following steps: a) Search for values of every component of the matching network; b) calculate minimum isolation and minimum return loss of the circulator device over the frequency range f_a to f_b for every solution and plot these isolations and return losses on a Pareto population chart; c) choose a design point from the chart that meets the specified requirements.

By applying this algorithm to the 400 MHz crossover network associated with Eq. (30), we obtain the Pareto population chart shown in Figure 8. The optimal matching network associated with this chart is chosen and the corresponding component values are

$$\begin{aligned} C_0 &= 2.13\,\text{pF} \\ C_g &= 40.2\,\text{pF} \\ C_1 &= 5.98\,\text{pF} \\ L_1 &= 82.9\,\text{nH} \\ R_L &= 189.3\,\Omega. \end{aligned} \tag{34}$$

The corresponding frequency response of this circulator device is shown in Figure 9. A performance with 15 dB isolation, 15.1 dB return loss and 0.3 dB insertion loss is obtained over the frequency band 136 MHz to 400 MHz, which is consistent with the 194% bandwidth predicted by Eq. (30) previously.

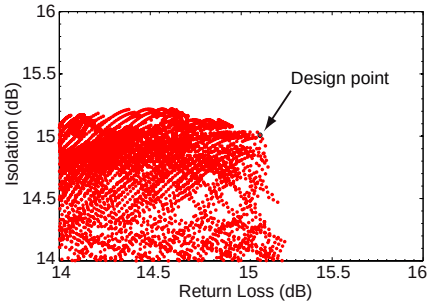

Figure 8. A Pareto population chart showing of all possible matching network solutions.

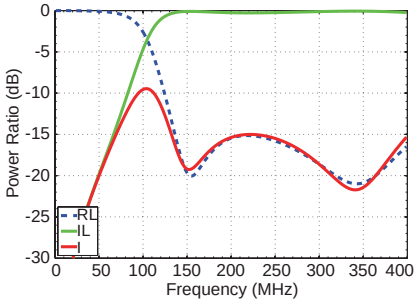

Figure 9. Frequency response of an ideal circulator optimized for widest bandwidth when f_b = 400 MHz.

3. ACTUAL CIRCULATOR DEVICE OPTIMIZATION

The previous section provides the necessary insight on wide-band operation of a ferrite circulator using an ideal model. For actual circulator hardware the model fails, but the bandwidth optimizing procedure (i.e., using the circulation impedance as a metric to determine bandwidth) is still applicable. For actual hardware, a better model, and hence a better estimate of the Z-parameters, can be obtained from numerical simulation. Following the same procedure developed for the ideal model, we discovered through simulation that a bandwidth of 125% (i.e., 178–400 MHz) is indeed possible when $4\pi M_s = 3275$ G. When fabricated and tested, we measured a 129% bandwidth (175–400 MHz). Figure 10 shows a picture of the fabricated circulator and the HFSS simulation model. The frequency response comparison between data obtained from measurement and simulation is shown in Figure 11. Although both simulation and experimental data failed to achieve the ideal value of 194%, this is to be expected

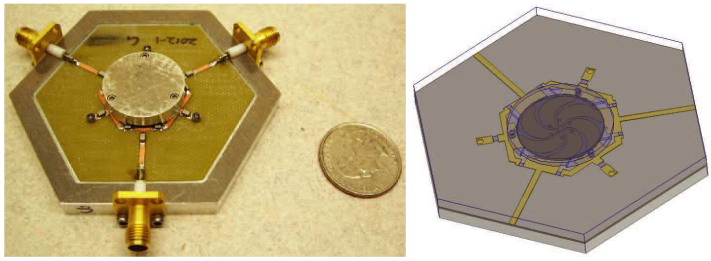

Figure 10. The fabricated circulator device and the HFSS model.

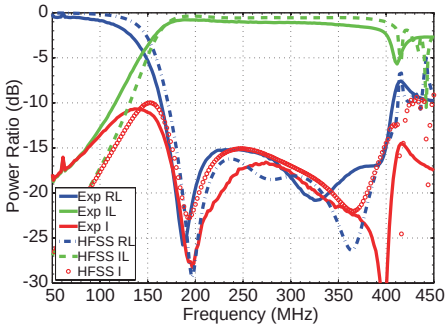

Figure 11. Frequency response comparison between data obtained from experiment (Exp) and from simulation (HFSS) when $f_b = 400$ MHz.

due to the many deficiencies associated with the ideal model. More importantly, the optimizing method proved to be a success by achieving unprecedented bandwidth performance.

4. CONCLUSION

In this paper we discussed the optimization procedure for bandwidth enhancement of an ideal crossover circulator. We demonstrated that 194% bandwidth is theoretically obtainable by optimizing both the crossover structure and matching network. By using frequency-normalization techniques, we show that the method is fully general for any above-FMR circulator. Moreover, by using this same method along with simulation tools, we were able to achieve bandwidths on the order of 130%, as validated in hardware. The difference between the theoretical performance verses the hardware performance is directly traceable to the deficiencies of the ideal model (e.g., uniform field assumption).

ACKNOWLEDGMENT

This work was supported by the Office of Naval Research under grant number N00014-08-1-0286. The authors give special thank to Dr. Jeffrey Allen of Navy SPAWAR, San Diego, CA for his comments and suggestions.

REFERENCES

1. Konishi, Y., "Lumped element Y circulator," *IEEE Trans. MTT*, Vol. 13, No. 6, 852–864, 1965.
2. Konishi, Y., "New theoretical concept for wide band gyromagnetic devices," *IEEE Trans. Magnetics*, Vol. 8, No. 3, 505–508, 1972.
3. Anderson, L., "An analysis of broadband circulators with external tuning elements," *IEEE Trans. MTT*, Vol. 15, No. 1, 42–47, 1967.
4. Miura, T., M. Kobayashi, and Y. Konishi, "Optimization of a lumped element circulator based on eigenvalue evaluation and structural improvement," *IEEE Trans. MTT*, Vol. 44, No. 12, 2648–2654, 1996.
5. Schloemann, E. F., "Circulators for microwave and millimeter-wave integrated circuits," *Proceedings of the IEEE*, Vol. 76, No. 2, 188–200, 1988.
6. Bergman, J. O., "Equivalent circuit for a lumped-element Y circulator," *IEEE Trans. MTT*, Vol. 16, No. 5, 308–310, 1968.

7. Polder, D., "On the theory of ferromagnetic resonance," *Phil. Mag.*, Vol. 40, 99–115, 1949.
8. Knerr, R. H. and C. E. Barnes, "A compact broad-band thin-film lumped element L-band circulator," *IEEE Trans. MTT*, Vol. 18, No. 12, 1100–1108, 1970.
9. Knerr, R. H., "An improved equivalent circuit for the thin-film lumped element circulator," *IEEE Trans. MTT*, Vol. 20, No. 7, 446–452, 1972.
10. Young, J. L., R. S. Adams, B. O'Neil, and C. M. Johnson, "Bandwidth optimization of an integrated microstrip circulator and antenna assembly: Part 2," *IEEE Antennas and Propagation Magazine*, Vol. 49, No. 1, 82–91, 2007.
11. Allen, J. C., *H^∞ Engineering and Amplifier Optimization*, Birkhäuser, Boston, MA, 2004.
12. Krowne, C. M. and R. E. Neidert, "Theory and numerical calculations for radially inhomogeneous circular ferrite circulators," *IEEE Trans. MTT*, Vol. 44, No. 3, 419–431, 1996.
13. Young, J. L. and C. M. Johnson, "A compact, recursive trans-impedance Green's function for the inhomogeneous ferrite, microwave circulator," *IEEE Trans. MTT*, Vol. 52, No. 7, 1751–1759, 2004.
14. Joseph, R. I. and E. Schlomann, "Demagnetizing field in nonellipsoidal bodies," *Journal of Applied Physics*, Vol. 36, No. 5, 1579–1593, 1965.
15. Wu, Y. S. and F. J. Rosenbaum, "Wide-band operation of microstrip circulators," *IEEE Trans. MTT*, Vol. 22, No. 10, 849–856, 1974.